2017

Optical conductivity of a commensurate graphene-topological insulator heterostructure

Matthew Sanderson
University of Wollongong, msanders@uow.edu.au

Sunchao Huang
University of Wollongong, sh676@uowmail.edu.au

Qiaoliang Bao
Monash University

C Zhang
University of Wollongong, czhang@uow.edu.au

Optical conductivity of a commensurate graphene-topological insulator heterostructure

Abstract

The optical conductivity of a heterostructure formed by a commensurate stacking of graphene and a topological insulator (TI) is investigated using the Kubo formalism. Both the intra- and interband AC conductivities are found to be sensitive to the graphene-TI coupling. The direct interband transition in graphene which is the origin of the universal conductance is forbidden due to the topological nature is the coupling. Furthermore, the graphene-TI coupling gives rise to additional broken symmetries, resulting in both the inter- and intraband conductivity to be reduced in the graphene-TI heterostructure. By varying the Fermi energy of the heterostructure, the band that gives the largest contribution changes, which in turn affects the overall electronic transport.

Publication Details

Sanderson, M., Huang, S., Bao, Q. & Zhang, C. (2017). Optical conductivity of a commensurate graphene-topological insulator heterostructure. Journal of Physics D: Applied Physics, 50 (38), 385301-1-385301-5.

Optical conductivity of a commensurate graphene-topological insulator heterostructure

Matthew Sanderson[1], Sunchao Huang[1], Qiaoliang Bao[2], Chao Zhang[1]

[1] *School of Physics, University of Wollongong, Northfield Avenue, New South Wales 2522, Australia and*

[2] *Department of Materials Science and Engineering, Monash University, Wellington Road, Clayton, Victoria 3800, Australia*

The optical conductivity of a heterostructure formed by a commensurate stacking of graphene and a topological insulator (TI) is investigated using the Kubo formalism. Both the intra- and interband AC conductivities are found to be sensitive to the graphene-TI coupling. The direct interband transition in graphene which is the origin of the universal conductance is forbidden due to the topological nature is the coupling. Furthermore, the graphene-TI coupling gives rise to additional broken symmetries, resulting in both the inter- and intraband conductivity to be reduced in the graphene-TI heterostructure. By varying the Fermi energy of the heterostructure, the band that gives the largest contribution changes, which in turn affects the overall electronic transport.

Topological insulators (TI's) have been widely studied particularly with respect to semiconducting heterostructures, formation of interface states and topological quantum Hall edge states[1–4]. The surface states of a topological insulator are found to have a linear low energy dispersion[5], known as a Dirac point, similar to the dispersion for monolayer graphene. In both systems near the Dirac point, the massless two-dimensional chiral fermionic excitations are characterized by the interlocking of spin (or quasi-spin) and the momentum. Both graphene and topological insulators have also been theorised to exhibit large magneto-optical effects[6,7] which can affect the conductivity and result in Kerr rotation. There does however exist qualitative differences between these two types of massless Dirac Fermions, chief among them is that the quantum spin Hall effect only exists in the surface states of TI's. Due to the linear dispersion relation around the Dirac point there has been a considerable amount of interest in the optical properties of the aforementioned two-dimensional systems[8]. It is yet to be seen however, what effect there is on the optical properties of a system whereby a coupling occurs between these two similar two-dimensional systems. Recently it has been shown[9] that such a TI-graphene heterostructure can be fabricated. It is expected that the weak spin-orbital coupling (SOC) in graphene can be enhanced by the proximity effect in TI-graphene heterostrctures[10–12]. Theoretical work[13] showed a significant enhancement of the SOC in graphene which can be further controlled by the relative rotation of the graphene lattice and the TI lattice.

The optical properties of graphene and topological materials in the terahertz to far infrared regime has been a topic of some interest due to the ongoing search for viable terahertz detectors and emitters, as well as the ubiquitous research being undertaken within the infrared frequencies used for telecommunications purposes. Due to the tunable Fermi levels in these systems, the optical properties such as conductance and plasmon frequency can be tuned in a wide range. The linear energy dispersion can also give rise to a strong nonlinear response in both graphene and TI's[14–16]. A new graphene-Bi_2Te_3 heterostructure formed by growing Bi_2Te_3 on the graphene template has been fabricated to study the coupled 2D plasmons. It has been found that the extinction spectra of the graphene-Bi_2Te_3 heterostructure is three times greater in magnitude than that of graphene[17].

In this work we investigate the intra- and interband optical conductivity of a TI-graphene heterostructure. In what follows we shall show that the band hybridization blocks the direct band-to-band transition between the graphene bands. The total conductivity of the heterostructure decreases significantly when compared to the case where the graphene and TI are separated. This effect is

independent of the graphene-TI coupling strength and due to the topological nature. The formalism is based on the Kubo formula of conductivity and a constant relaxation rate is assumed. The results found highlight the effect of hybridisation of bands on the overall conductivity of a system. Individually the conductivities of the two systems are quite simple, but when brought together the conductivity exhibits quite complicated behavior. The conductivity calculated gives us a clearer picture of the optical properties of the material, as well as potentially allowing for creation of devices utilising these properties.

We consider a graphene-TI structure where the stacking is commensurate. It has been determined[5] that for Bi_2Se_3, Bi_2Te_3, and Sb_2Te_3 compounds, the surface states are on the 111 surface. The projected surface Brillouin zone (BZ) is hexagonal with a single DP at the zone center[5]. The Dirac points of the graphene monolayer will line up quite closely to the Dirac points of the topological insulator due to the difference in sizes in the crystal structures. Due to the overlap of Brillouin zones, a direct coupling between Dirac cones is possible. The structure is a $\sqrt{3} \times \sqrt{3}$ stacked graphene BZ and TI BZ in the repeated zone scheme and the model Hamiltonian is given in the following form[13],

$$\hat{\mathcal{H}} = \begin{pmatrix} \hat{H}^{g,K}_{\mathbf{k}} & 0 & \hat{T}^{\dagger} \\ 0 & \hat{H}^{g,K'}_{\mathbf{k}} & \hat{T}^{\dagger} \\ \hat{T} & \hat{T} & \hat{H}^{TI}_{\mathbf{k}} \end{pmatrix} \tag{1}$$

where $\hat{H}^{g,K} = v_F^g \begin{pmatrix} 0 & 0 & 0 & p_- \\ 0 & 0 & p_- & 0 \\ 0 & p_+ & 0 & 0 \\ p_+ & 0 & 0 & 0 \end{pmatrix}$ and $\hat{H}^{g,K'} = \left(\hat{H}^{g,K}\right)^{\dagger}$ are the (4×4) Hamiltonians for graphene at the K and K' points respectively (including spin degeneracy), $\hat{H}^{TI} = iv_F^{TI} \left(\begin{smallmatrix} 0 & p_- \\ p_+ & 0 \end{smallmatrix}\right)$ is the Hamiltonian for the surface of a topological insulator without a gap, and $\hat{T} = \left(\begin{smallmatrix} t & 0 & 0 & 0 \\ 0 & t & 0 & 0 \end{smallmatrix}\right)$ is a coupling term describing hopping between the graphene layer and the TI surface. $p_\pm = p\mathrm{e}^{\pm i\theta} = \hbar(k_x \pm ik_y)$, and v_F^g and v_F^{TI} are the Fermi velocity for the graphene and topological insulator layers respectively, and $t = 0.05$eV is the inter-layer hopping energy[13]. The basis vector for Eq. (1) contains terms for creation of massless Dirac fermions on both sublattices in the graphene lattice for both valleys and spins (accounting for the first $2 \times 2 \times 2 = 8$ terms), and the creation of a surface massless fermion with spin on the topologically insulating surface (accounting for a further 2 terms). While the Hamiltonians are usually not linked, by including a hopping term between the two layers, there

is an intermingling of terms entering through the $\hat{T}$ operator.

This Hamiltonian includes both K and K' valleys of graphene, as well as the spin state of electrons which are both normally ignored and added as degeneracies ($g_v = 2$ and $g_s = 2$ respectively).

By diagonalising the Hamiltonian we can find an implicit form of the energy dispersion for this system

$$(E + v_g p)^2 (E - v_g)^2 \left(E^3 - v_{TI} p E^2 - (2t^2 + v_g^2 p^2) E + v_{TI} v_g^2 p^3\right) \times \left(E^3 + v_{TI} p E^2 - (2t^2 + v_g^2 p^2) E - v_{TI} v_g^2 p^3\right) = 0 \quad (2)$$

where $v_g = v_F^g$ and $v_{TI} = v_F^{TI}$. We will be using the familiar value of $v_F^g \approx 1 \times 10^6$m/s, and we will approximate $v_{TI} = \frac{1}{2} v_g$ due to the difference in sizes of the physical structures of graphene and topological insulators[13].

It can be seen from Eq. (2) that the usual graphene band structure still remains, but with a degeneracy of 2 instead of 4 as would be expected when considering valley and spin degeneracy. The energy dispersion shown in Fig. 1 is the same as that presented in Ref.[10]. We redraw it here with explicit band labelling to assist our discussion of various electronic transitions and optical conductivity.

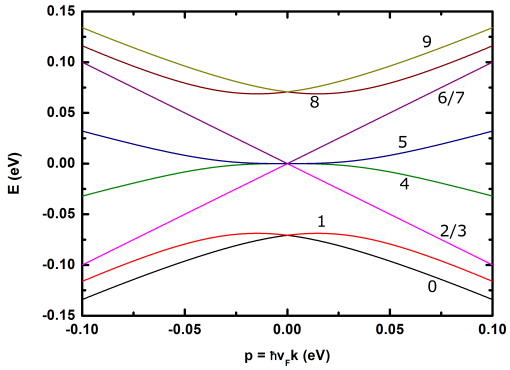

FIG. 1: Energy band structure for $t = 0.05$eV. The bands are numbered from bottom to top as a convenient referencing system. Both graphene bands have two numbers due to their 2-fold degeneracy.

The lowest point of the upper bands is at $E_{min} = \frac{3\sqrt{6}t}{\sqrt{10+7\sqrt{7}}}$, and the crossing point of the two upper bands is at $E_c = \sqrt{2}t$. As we will be calculating the conductivity at zero temperature, sharp changes are expected to occur at these points. The upper splitting of the bands is a Rashba-like splitting and the size of this can be written as $\Delta_R = E_c - E_{min}$.

We write the velocity operators using $\hat{v}_\nu = \frac{1}{\hbar}\frac{\partial \hat{\mathcal{H}}}{\partial k_\nu} = \frac{\partial \hat{\mathcal{H}}}{\partial p_\nu}$.

$$\hat{v}_\nu = \begin{pmatrix} \hat{v}_\nu^K & 0 & 0 \\ 0 & \hat{v}_\nu^{K'} & 0 \\ 0 & 0 & \hat{v}_\nu^{TI} \end{pmatrix} \tag{3}$$

This system exhibits an interesting property that in partially breaking the degeneracy of the graphene bands, the remaining degenerate graphene bands are actually hybridised from the original valley degenerate bands[13]. Due to this hybridisation of two orthogonal states, transitions between the two different graphene bands are forbidden, ie.

$$\langle \psi_{g,s}^{\alpha} | v_x | \psi_{g,s'}^{\alpha'} \rangle = 0 \tag{4}$$

for $s, s' = \uparrow$ or $\downarrow$, and $\alpha \neq \alpha'$. The hybridisation is such that $\psi_{g,s}^{\alpha} = \frac{1}{\sqrt{2}}\left(\psi_{K,s}^{\alpha} - \psi_{K',s}^{\alpha}\right)$ where the wavefunctions on the right are those for an isolated graphene sheet. It is straightforward to show that the berry phase of the two graphene bands is zero as compared to π of an isolated graphene sheet.

Based on these electronic properties, we calculate the frequency dependent conductivity of the system. From the Kubo formula the intraband conductivity can be written in the form,[18]

$$\sigma_{\mu\nu}^{intra} = \frac{i g_s g_v \sigma_0}{\pi^2} \sum_\lambda \int p \, \mathrm{d}p \, \mathrm{d}\theta \delta(E_\lambda(p) - E_F) \frac{\langle \psi_\lambda | v_\mu | \psi_\lambda \rangle \langle \psi_\lambda | v_\nu | \psi_\lambda \rangle}{\xi + i\gamma_\lambda} \tag{5}$$

where the summation runs over the band index, λ, $\xi = \hbar\omega$ and $\gamma_\lambda = \hbar/\tau_\lambda$. Eq.(5) ignores the details of the electron scattering and electron-electron correlation in transport[19] and assumes a constant relaxation rate per band, γ_λ. As all spin and valley degeneracies are included explicitly in the Hamiltonian we have that $g_s = g_v = 1$. For the relaxation rate, γ_λ we will use one value for all

the bands, $\gamma = \gamma_\lambda = 2.6$meV and neglect the frequency dependency. This value for the relaxation rate is assigned arbitrarily, so we pick the value that has been used for graphene[20] previously, allowing us to compare the results between the two systems more easily. The actual value for the system will of course vary from the value in graphene, and will vary by individual band within the structure. The primary effect this value has on the result is peak broadening, so the details of the result will still be valid, irrespective of our chosen value for γ.

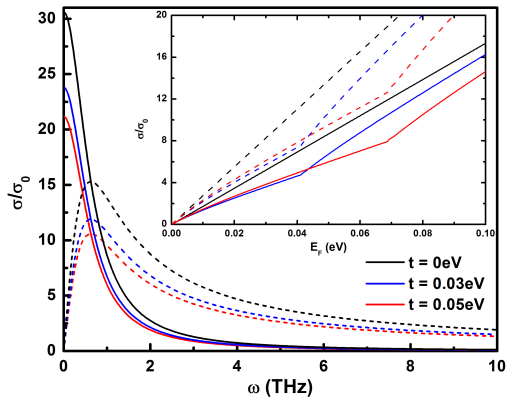

FIG. 2: Intraband conductivity vs frequency at $E_F = 0.05$eV at various coupling parameters. Inset: Conductivity vs Fermi energy with $\omega = 1$THz. Solid and dashed lines correspond to the real and imaginary components respectively.

Fig. 2 shows the longitudinal intraband conductivity in terms of $\sigma_0 = \frac{e^2}{4\hbar}$. The main panel is the frequency dependence. The zero-frequency limit represents the Drude weight. As the graphene-TI coupling increases, the Drude weight decreases. Since the Drude weight for an isolated system is inversely proportional to the scattering rate, the reduction of the Drude weight in the coupled system is due to the additional hopping between the two layers in the system. The carrier can be relaxed via scattering or via interlayer hopping.As the coupling increases, the TI band (band 5) flattens further. For samples with fixed carrier concentration, the Fermi level decreases because the density of states increases as band flattens. This will result in a further decrease of the conductivity as t increases. The inset of Fig. 2 shows the dependence of the conductivity on the Fermi level. The intraband conductivity increases with the Fermi level. When the Fermi level touches the bottom of band 8 where the density of states is highest, the conductivity gains a sudden extra source. As a result a kink is seen at $E_F = E_{min}$ and $E_F = E_c$.

We note that the structure considered here consists of two pure 2D Dirac systems coupled together through the interlayer hopping. In principle there is a k_z-dependence since the interlayer hopping is along the z-direction. However, such dependence is now implicitly included in the hopping parameter. A large interlayer separation means a small t. The electromagnetic response is purely 2D, i.e, the electrons only respond to the field polarising along the plane. A field component along the z-direction will modify the interlayer hopping. Since hopping is a parameter in this model, the transport along the 2D plane can be viewed as dependent on the z-component of the field through the parameter t.

The interband conductivity can be calculated in the same manner,[18]

$$\sigma_{\mu\nu}^{inter} = \frac{i\hbar e^2}{4\pi^2} \sum_{\lambda \neq \lambda'} \int p \, \mathrm{d}p \, \mathrm{d}\theta \frac{(f_\lambda - f_{\lambda'}) \langle \psi_\lambda | v_\nu | \psi_{\lambda'} \rangle \langle \psi_{\lambda'} | v_\mu | \psi_\lambda \rangle}{(E_\lambda - E_{\lambda'}) (E_\lambda - E_{\lambda'} + \hbar\omega + i\gamma_\lambda)} \tag{6}$$

Where we sum over inequivalent bands.

Fig. 3 shows the frequency dependent interband conductivity. This rich structure of the frequency dependency reflects the contribution of various interband transitions allowed at a given Fermi level.

Various peaks and steps in the conductivity curves are related to the transitions between specific bands. The highest peak is due to the transition between the states with highest density of states, for example the transition from band 4 to band 8. We have analyzed and identified specific transitions associated with the steps in conductivity. For example, at $E_F = 0.05$ the steep step around 10THz is due to the transition from the lowest TI band (5) to the lowest graphene band (6/7). The same step occurs at around 12THz for $E_F = 0.07$eV and around 15THz for $E_F = 0.09$eV. Steps in the real part of the conductivity become dips in the imaginary part of the conductivity, therefore all dips can be assigned to a given interband transition based on the energy dispersion of Fig. 1. This is shown in Fig. 3(b).

It can be seen in Fig. 3 that changing the Fermi energy will cause a drastic change in the conductivity curves as the location or possibility of the resonances vary with the size of the Fermi energy.

In the high frequency limit, the real part of the conductivity approaches as constant value of $\frac{5}{4}\sigma_0$.

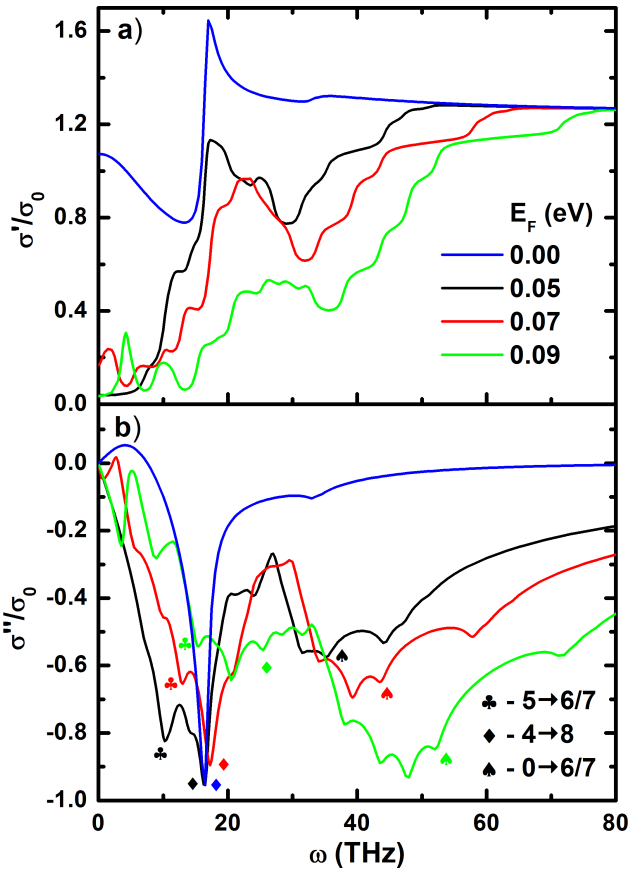

FIG. 3: The interband conductivity vs frequency at various Fermi energies, the coupling parameter is $t = 0.05$eV. (a) the real part, and (b) the imaginary part.

The conductivity of $\frac{5}{4}\sigma_0$ is significantly lower that the sum of two universal conductances, $2\sigma_0$, for the decoupled two Dirac systems. This is mainly due to the fact that the direct transitions between the two graphene-like bands is forbidden. Secondly, due to the hopping breaking the degeneracies of the graphene layer and modifying the band structure, the resultant bands give a lower contribution to the conductivity due to their flatter shape.

In Fig. 4, we show the Fermi energy dependent conductivity at low frequencies. We now analyze the Fermi level dependence of the real part of the interband conductivity. The imaginary part can be understood through the Kramars-Kronig relations. At zero frequency (black line) the transition energy is zero and the only possible transitions are around the Dirac points. There are two Dirac points, one at $E = 0$, and the other at $E = \sqrt{2}t$. When the Fermi level is around either of these

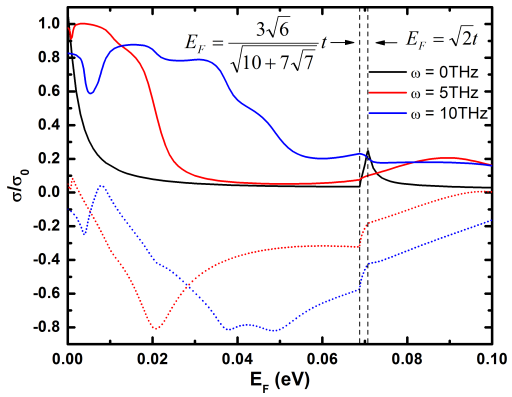

FIG. 4: Interband conductivity vs the Fermi energy for a range low frequencies. The solid lines are the real parts and the dotted lines are the imaginary parts. At zero frequency, the conductivity is purely real. The coupling is $t = 0.05$eV.

two points, an absorption peak occurs. Away from the Dirac points, the absorption is negligible but non-zero due to the finite relaxation rate γ. For $\omega = 10$THz (blue line), the transition probability is finite everywhere. At zero E_F, three transitions are allowed; the $2/3 \to 5$ and $4 \to 6/7$ transitions, both at the same momentum (p_1), and the $4 \to 5$ transition which is at a higher momentum (p_2 where $E_5(p_2) - E_4(p_2) = \hbar(10\text{THz})$). The total strength of these transitions is weaker than the $4 \to 5$ transition at zero momentum (ie. $E_F = 0$) since the density of states diverges for bands 4 and 5 at zero momentum. As a result, the conductivity is slightly lower at $\omega = 10$THz than at zero frequency. As E_F increases, the $4 \to 5$ transition, for example, is no longer possible at 10THz as the upper energy states are now filled at $p = p_2$, causing the conductivity to decrease. This decrease with increasing E_F is offset by the increase in conductivity due to new transitions contributing (for example $4 \to 6$). This gives rise to the complex structure of the conductivity as seen in Figs. 3 and 4. With the help of the energy dispersion (Fig. 1), we can identify which transition are allowed and which are disallowed as E_F and ω vary. By decomposing the conductivity into contributions due to individual band transitions the complicated E_F dependence of the conductivity can be understood qualitatively and quantitatively.

In summary we have calculated the frequency and Fermi energy dependence of the optical conductivity in a graphene-TI heterostructure. The transport is strongly dependent on the graphene-TI coupling. By allow hopping between the two commensurate layers, the total conductivity is in

general decreased compared to the total conductivity found by naively adding the graphene and topological insulator conductivities together. This is due to a direct interband transition being forbidden between the two hybridised graphene bands. Hybridisation of bands as well as lifted degeneracies results in a complex band structure, which in turn leads to an optical conductivity with a large number of features.

The frequency dependence of the interband conductivity is considerably more complex than the case for the two system separately due to the far larger number of possible transitions between bands, and thus many more resonances are possible. If the hopping strength between layers could be modified it would create a way to vary the conductivity, allowing for direct tuning of electronic transport though the material. This in-depth investigation into the conductivity could also be used to determine and understand the plasmonic properties of the material.

Finally we note that in this work we only considered the case of commensurate stacking and a gapless TI surface state. Going beyond these two assumptions and calculating the conductivity for an incommensurate stacking or a gapped graphene-topological insulator stacking will result in a more complicated band structure[21–23] and could lead to further interesting electronic transport properties. It is possible that the restricted interband transition between the two graphene-like bands could be lifted in either of these cases, potentially leading to an increase in conductivity.

ACKNOWLEDGMENTS

This work was supported by the Australian Research Council Discovery Grant (DP140101501).

REFERENCES

[1]B. A. Bernevig, T. L. Hughes, and S. C. Zhang, Science **314**, 1757 (2006).

[2]M. König, S. Wiedmann, C. Brüne, A. Roth, H. Buhmann, L. W. Molenkamp, X. L. Qi, and S. C. Zhang, Science **318**, 766 (2007).

[3]G. M. Gusev, E. B. Olshanetsky, Z. D. Kvon, N. N. Mikhailov, S. A. Dvoretsky, and J. C. Portal, Phys. Rev. Lett. **104**, 166401 (2010).

[4]K. C. Nowack, E. M. Spanton, M. Baeninger, M. König, J. R. Kirtley, B. Kalisky, C. Ames, P.

Leubner, C. Brune, H. Buhmann, L. W. Molenkamp, D. Goldhaber-Gordon, and K. A. Moler, Nat. Mater. **12**, 787 (2013).

[5]H. J. Zhang, C. X. Liu, X. L. Qi, X. Dai, Z. Fang, and S. C. Zhang, Nat. Phys. **5**, 438 (2009).

[6]V. Gusynin, S. Sharapov, and J. Carbotte. J. Phys.: Condensed Matter, **19**, 026222 (2006).

[7]W. K. Tse and A. MacDonald. Phys. Rev. Lett. **105**, 057401 (2010).

[8]V. Vargiamidis and P. Vasilopoulos, J. Appl. Phys. **116**, 063713 (2014).

[9]G. Bian et al., 2D Materials **3**, 021009 (2016)

[10]W. H. Dang, H. L. Peng, H. Li, P.Wang, and Z. F. Liu, Nano Lett. **10**, 2870 (2010).

[11]C.-L. Song, Y.-L. Wang, Y.-P. Jiang, Y. Zhang, C.-Z. Chang, L. Wang, K. He, X. Chen, J.-F. Jia, Y. Wang et al., Appl. Phys. Lett. **97**, 143118 (2010).

[12]K. H. Jin and S. H. Jhi. Physical Rev. B **87**, 075442 (2013).

[13]J. Zhang, C. Triola, and E. Rossi, Phys. Rev. Lett.,**112**, 096802 (2014).

[14]A. R. Wright, X. G. Xu, J. C. Cao, and C. Zhang, Appl. Phys. Lett. **95**, 072101 (2009)

[15]Yee Sin Ang, Shareef Sultan, and C. Zhang, Appl. Phys. Lett. **97**, 243110 (2010)

[16]Qinjun Chen, Yee Sin Ang, R. A. Lewis, Xiaolin Wang, and Chao Zhang, Appl. Phys. Lett. **101**, 211109 (2012)

[17]Y. Lu et al., J. Opt. Soc. Amer. **33**, 1842 (2016).

[18]L. A. Falkovsky and A. A. Varlamov, European Physical Journal B, **56**, 281 (2007)

[19]C. Zhang and N. Tzoar, Phys. Rev. A **38**, 5786 (1988))

[20]Yu. V. Bludov, A. Ferreira, N. M. R. Peres and M. I. Vasilevskiy, International Journal of Modern Physics B, **27**, 10 (2013).

[21]K. S. Novoselov, D. Jiang, F. Schedin, T. J. Booth, V. V. Khotkevich, S. V. Morozov, and A. K. Geim, Proc. Natl. Acad. Sci. U.S.A. **102**, 10451 (2005).

[22]S. Kim, J. Nah, I. Jo, D. Shahrjerdi, L. Colombo, Z. Yao, E. Tutuc, and S. K. Banerjee, Appl. Phys. Lett. **94**, 062107 (2009).

[23]S. Kim, I. Jo, J. Nah, Z. Yao, S. K. Banerjee, and E. Tutuc, Phys. Rev. B **83**, 161401 (2011).